

Phosphinidene Transition Metal Complexes: A Combined Ab Initio MO-DFT Study of $\text{Cr}(\text{CO})_5\text{-PR}$

Steven Creve,^[a] Kristine Pierloot,^[a] Minh Tho Nguyen,^{*[a]} and Luc G. Vanquickenborne^[a]

Keywords: Ab initio calculations / Density functional calculations / Phosphinidene / Carbonyl complexes

Ab initio MO and DFT calculations have been performed on phosphinidene complexes of the type $\text{Cr}(\text{CO})_5\text{-PR}$, with $\text{R} = \text{H}, \text{CH}_3, \text{SiH}_3, \text{NH}_2, \text{PH}_2, \text{OH},$ and SH . The formation of the Cr–P bond essentially arises from a ligand-to-metal charge transfer. While a significant π backdonation is also observed for the $\text{Cr}(\text{CO})_5\text{-PH}$, $\text{Cr}(\text{CO})_5\text{-PCH}_3$, and $\text{Cr}(\text{CO})_5\text{-PSiH}_3$ complexes, this is less the case for $\text{Cr}(\text{CO})_5\text{-POH}$, $\text{Cr}(\text{CO})_5\text{-PSH}$, and $\text{Cr}(\text{CO})_5\text{-PNH}_2$, and the backbonding almost disappears for $\text{Cr}(\text{CO})_5\text{-PPH}_2$. In both the lowest lying singlet

and triplet states, all complexes exhibit a staggered conformation. CASSCF/CASPT2 calculations performed with the ANO basis sets indicate a closed-shell singlet ground state along the whole series. The binding energy between $\text{Cr}(\text{CO})_5$ and PR ranges from 216 kJ/mol for $\text{Cr}(\text{CO})_5\text{-PNH}_2$ to 127 kJ/mol for $\text{Cr}(\text{CO})_5\text{-PSiH}_3$ (B3LYP values). In general, the B3LYP-DFT scheme yields reasonable qualitative and quantitative results when compared with CASPT2(12/12).

1 Introduction

Phosphinidenes (R-P) are known as important transient species in phosphorus chemistry that can be stabilized through complexation with transition metal fragments. In contrast to analogous transient intermediates such as carbenes, nitrenes, and silylenes, spectroscopic information on free phosphinidenes is rather scarce. In fact, the ESR spectrum of an aryl derivative (Mes-P) has only recently been recorded.^[1] In most cases, these short-lived and highly reactive species have been trapped in transition metal complexes and can be used in this way as starting materials in organophosphorus syntheses.^[2]

Recently, we^[3–6] and others^{[7][8]} have shown by high-level ab initio calculations, that phosphinidenes exhibit an inherent triplet electronic ground state but that the singlet counterparts can be stabilized strongly by substituents through both electronic and steric effects. For example, amino ($\text{R}_2\text{N-P}$) and phosphino ($\text{R}_2\text{P-P}$) derivatives containing large alkyl groups are likely to possess a closed-shell singlet ground state.^[3]

Mathey^{[9][10]} and Lammertsma^[11] suggested from numerous experimental observations of the complexed species that the phosphinidene ligand within the coordination sphere of a metal fragment behaves as a typical singlet monovalent intermediate giving a higher and cleaner reactivity. Nevertheless, the identity of the ground state of complexed phosphinidenes still remains an open question.

To our knowledge, only three theoretical studies of terminal phosphinidene complexes have yet been reported. The first one dealt with an Extended Hückel study of a number of substituted phosphinidene ligands (PCH_3 , PNH_2 , PPH_2 , ...).^[12] Idealized geometries were used

throughout, based on parameters chosen from experimental data on parent species. Although very useful, this study only yields a qualitative picture of the considered complexes. In two other studies, partial geometry optimizations of the $\text{Cr}(\text{CO})_5\text{-PH}$ complex were performed.^{[13][14]} However, the P–Cr bond length turned out to be 1.9 Å at the Extended Hückel level^[13] while it was found to be 2.33 Å by ROHF calculations.^[14] Disagreement concerning the singlet or triplet nature of the ground state of $\text{Cr}(\text{CO})_5\text{-PH}$ also arose. In our previous study on $\text{Cr}(\text{CO})_5\text{-PH}$,^[15] high-level ab-initio calculations have been applied, removing these discrepancies. We showed that $\text{Cr}(\text{CO})_5\text{-PH}$ has a singlet ground state with a P–Cr distance of 2.268 Å. The lowest lying triplet was 35 kJ/mol higher in energy. In this work, an extension is made to $\text{Cr}(\text{CO})_5$ complexes of different phosphinidenes PR, yielding a deeper understanding of the singlet-triplet energy problem in these species. Furthermore, the backbonding phenomenon usually observed in metal complexes will be addressed, since it is not well characterized yet for phosphinidene complexes.^[16]

The theoretical study presented here, includes full geometry optimizations and high-level energy calculations on a series of simple carbonylchromium complexes, $\text{Cr}(\text{CO})_5\text{-PR}$, in which $\text{R} = \text{H}, \text{CH}_3, \text{SiH}_3, \text{NH}_2, \text{PH}_2, \text{OH},$ and SH .

2 Details of the Calculations

2.1 Computational Methods

All geometries were fully optimized with density functional theory, using the B3LYP functional^{[17][18]} in combination with 6-31G(d,p) basis sets for all atoms, except for Cr. For the latter element we used a (14s,9p,5d)/[8s,5p,3d] basis set,^[19] augmented by two *p*-functions^[20] with exponents 0.120675 and 0.038610, one *d*-function^[21] with exponent 0.09720, and one *f*-function with exponent 1.0,

^[a] Department of Chemistry, University of Leuven, Celestijnenlaan 200F, B-3001 Leuven, Belgium.

Supporting information for this article is available on the WWW under <http://www.wiley-vch.de/home/eurjic> or from the author.

respectively. This $[8s,7p,4d,1f]$ basis set for Cr will be denoted hereafter as "TZ+2PDF".

In our preliminary study on the $\text{Cr}(\text{CO})_5\text{-PH}$ complex,^[15] it was found that the (U)HF, (U)MP2 or CASSCF/PT2(2/2) methods are not reliable in treating this kind of systems. Therefore, we now only consider the higher level CASSCF(12/12) and CASPT2(12/12) calculations, using the B3LYP optimized geometries. ANO basis sets were used^[22] for these calculations, following the contraction scheme shown below.

	primitive	contracted
H	7s3p	2s1p
C	10s6p3d	3s2p1d
N	10s6p3d	3s2p1d
O	10s6p3d	3s2p1d
Si	13s10p4d	4s3p2d
P	13s10p4d	4s3p2d
S	13s10p4d	4s3p2d
Cr	17s12p9d4f	6s4p3d1f

Our previous study^[15] pointed out that a more flexible contraction with the same primitive set does not significantly alter the results.

All B3LYP optimizations were performed using the Molliken software,^[23] while the CASSCF/CASPT2 calculations were done with the MOLCAS-4.0 code.^[24]

2.2 Notations

Figure 1 gives a schematic overview of the geometries for the different complexes and their proposed shorthand notations. For the $\text{Cr}(\text{CO})_5\text{-PH}$, $\text{Cr}(\text{CO})_5\text{-POH}$, and $\text{Cr}(\text{CO})_5\text{-PSH}$ complexes, two forms were considered, an "eclipsed" conformation, indicating that the P–R bond is eclipsed with one of the Cr–C_{eq} bonds, and a staggered form which has its P–R bond in between two Cr–C_{eq}

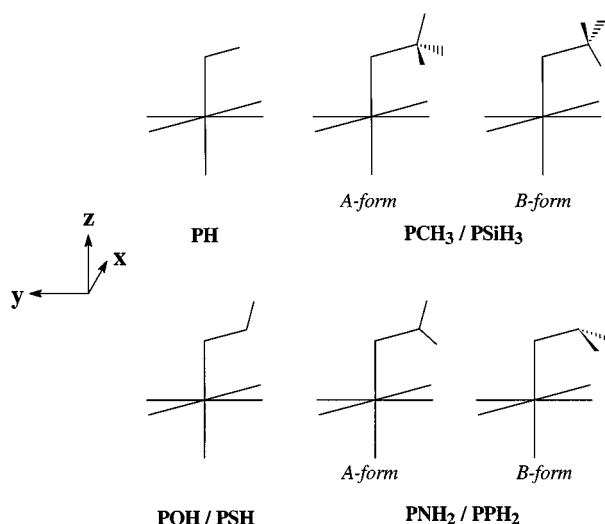


Figure 1. Schematic representation of the different $\text{Cr}(\text{CO})_5\text{-PR}$ complexes considered, along with the naming convention; only eclipsed forms are shown in this figure

bonds. For the $\text{Cr}(\text{CO})_5\text{-PCH}_3/\text{Cr}(\text{CO})_5\text{-PSiH}_3$ and $\text{Cr}(\text{CO})_5\text{-PNH}_2/\text{Cr}(\text{CO})_5\text{-PPH}_2$ cases, additional specifications are needed to indicate the rotational orientation of the CH_3/SiH_3 and NH_2/PH_2 groups, respectively. They are referred to as **A** and **B**, following the convention of Figure 1. As a shorthand notation for use in tables, we will, for instance, designate an eclipsed structure of the **A** type as **ec-A** and a staggered structure as **st-A**. Note from Figure 1 that the **B**-types of $\text{Cr}(\text{CO})_5\text{-PNH}_2$ and $\text{Cr}(\text{CO})_5\text{-PPH}_2$ have a pyramidal NH_2 or PH_2 unit, in contrast to their corresponding **A**-types.

2.3 Choice of the Active Space

The quality of a CASSCF calculation on a transition metal system critically depends on the choice of the active space. This space needs to include all valence orbitals necessary for an adequate description of the metal–ligand bonding. In a previous study,^[25] it was demonstrated that the ground state electronic structure of $\text{Cr}(\text{CO})_6$ is well described by a (10/10) space, built up from the metal 3d orbitals and their bonding and antibonding counterparts. For $\text{Cr}(\text{CO})_6$ this amounts to an occupied e_g (CO σ) and t_{2g} (Cr 3d) shell, and a virtual e_g (Cr 3d) and t_{2g} (CO π^*) shell. By replacing one CO ligand by a phosphinidene unit, however, an additional difficulty arises. The PR ligand has a triplet ground state with two singly occupied $p(\pi)$ orbitals. As a consequence, both π orbitals have to be added to the original (10/10) space. This means that the active space needed for an adequate description of $\text{Cr}(\text{CO})_5\text{-PR}$ consists of at least 12 electrons in 12 orbitals.

In the CASPT2 calculations, all valence electrons as well as the Cr semi-core 3s, 3p electrons were correlated, whereas the rest of the core (C, N, O 1s; Si, P, S 1s, 2s, 2p; Cr 1s, 2s, 2p) was kept frozen. Finally, first-order relativistic corrections (mass-velocity and Darwin term) have been added to the CASPT2 energies.

A remark has to be made for triplet **st-A** $\text{Cr}(\text{CO})_5\text{-PPH}_2$. In this case, it has not been possible to perform the CASSCF/PT2(12/12) calculation with the active space specified above. It turns out that one of the active orbitals (representing the Cr–P σ bond) spontaneously leaves the active space, in favor of the entering $3p_z(\text{Cr})$ orbital. Therefore, two additional calculations have been performed on the triplet **st-A** $\text{Cr}(\text{CO})_5\text{-PPH}_2$ species. The first was to force the calculation to keep the Cr–P σ bond in its active space, by freezing the orbitals during the CASSCF run up to $3p(\text{Cr})$. In another calculation, a reduced (10/11) space was used, containing neither the Cr–P σ bonding orbital, nor the $3p_z(\text{Cr})$ orbital. The relative energies obtained from both approaches differed by only 1.2 kJ/mol.

3 Results and Discussion

3.1 Electronic Structure

As quite a number of geometrical effects and properties of the relative energies cannot be fully understood without

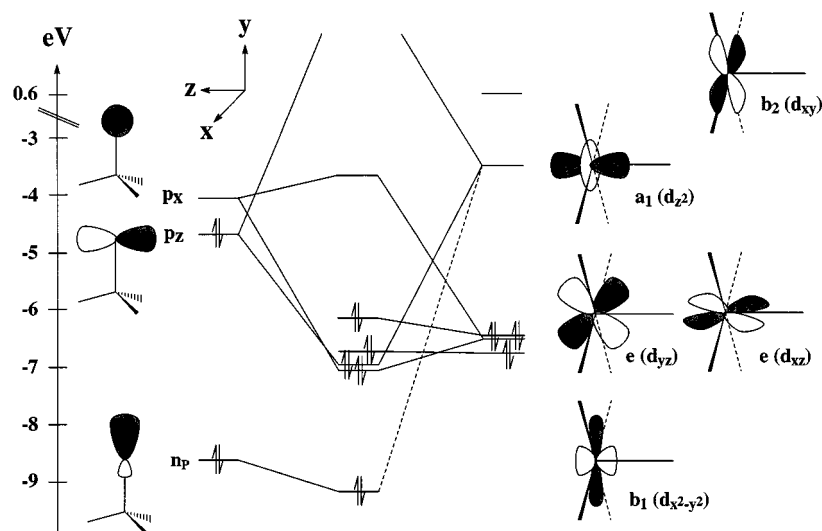


Figure 2. Schematic drawing of the orbital interactions in singlet **st-A** $\text{Cr}(\text{CO})_5\text{-PCH}_3$

having the electronic structure of the considered complexes in mind, the latter will be discussed first.

A careful analysis of the bonding situation in $\text{Cr}(\text{CO})_5\text{-PH}$ has already been reported.^[15] Therefore, we will recall briefly here the most important features. As a guideline, the orbital correlation diagram for the singlet **st-A** $\text{Cr}(\text{CO})_5\text{-PCH}_3$ complex shown in Figure 2, together with contour plots of the most important orbitals shown in Figure 3 are used in what follows. The highest occupied orbitals of the d^6 $\text{Cr}(\text{CO})_5$ fragment are the e orbitals (d_{xz} , d_{yz}) and a b_1 ($d_{x^2-y^2}$) orbital, which are stabilised through π backbonding with the empty CO π^* orbitals. The lowest unoccupied orbital is of a_1 symmetry (d_{z^2}), followed by a b_2 (d_{xy}) orbital. Both point directly towards the CO ligands and constitute the antibonding combinations arising from a σ -interaction with the CO 5σ orbitals. The PR molecule has a σ orbital directed along the P–R bond containing the phosphorus lone pair, n_p . Two phosphorus p orbitals, perpendicular to the P–R bond, contain another pair of electrons, usually in a triplet ground state configuration. However, the bonding is best understood by considering a singlet PR. In this case, one p orbital, perpendicular to the P–R bond and doubly occupied, is used to form a σ bond with the empty a_1 orbital of the $\text{Cr}(\text{CO})_5$ fragment. The remaining empty p_x orbital of PR is in an orientation suited to π backbonding with the doubly occupied $d_{xz}(\text{Cr})$ orbital. The antibonding combination arising from this interaction constitutes the LUMO of the resulting complex. For clarity, the phosphinidene complex in Figure 2 is represented with a Cr–P–R angle of 90° . Optimized structures, on the other hand, have an Cr–P–R angle of $105\text{--}130^\circ$. This can be understood by considering the secondary stabilizing interaction between the phosphorus n_p lone pair and the $d_{z^2}(\text{Cr})$ orbital (HOMO-4 of Figure 3) which increases if the Cr–P–R angle gets larger than 90° .

It is interesting to look at the evolution of the π backbonding through the series of complexes. Figure 4 shows

contour plots of the bonding orbital [with predominant $d_{xz}(\text{Cr})$ character] involved in the π backdonation. Immediately perceptible is the decrease of the $p_x(\text{P})$ orbital contribution in the series $\text{Cr}(\text{CO})_5\text{-PCH}_3 \rightarrow \text{Cr}(\text{CO})_5\text{-POH} \rightarrow \text{Cr}(\text{CO})_5\text{-PNH}_2$. The same trend is seen for the analogous series of second-row R groups. There, the decrease of the p orbital contribution is even more pronounced (an extreme case is shown as HOMO-1 of $\text{Cr}(\text{CO})_5\text{-PPH}_2$ in Figure 6). In order to have a more physical picture of the π backbond strength, density difference plots have also been made and are shown in Figure 5. This difference corresponds to the deformation density upon bond formation and is obtained as follows.

$$\Delta\rho = \rho_{\text{tot}}(\text{complex}) - [\rho_{\text{tot}}(\text{singlet PR}) + \rho_{\text{tot}}(\text{Cr}(\text{CO})_5)]$$

To compute $\Delta\rho$, the geometries of the fragments are frozen to their corresponding geometries in the complex. Full lines in Figure 5 correspond to an increase in total density, dotted lines to a decrease. As expected, one can see that charge is transferred from the $d_{xz}(\text{Cr})$ orbital to the $p_x(\text{P})$ orbital. Again, the extent of this charge transfer decreases as R varies in the order $\text{CH}_3 \rightarrow \text{OH} \rightarrow \text{NH}_2$. The same is also seen for the second-row series, but to a slightly higher extent. How can we understand such a weakening of the π back transfer? Table 1 shows the energy difference (ΔE) between the LUMO of the different PR fragments – the orbital which is involved in π backbonding – and the $d_{xz}(\text{Cr})$ orbital of $\text{Cr}(\text{CO})_5$. The larger the energy difference between both partners involved in the π bond, the weaker this bond. In more chemical terms, one could say that in PNH_2 , PPH_2 , POH , and PSH the empty phosphorus p_x orbital is already used by the neighboring heteroatom to delocalize its lone pair, making this orbital less available for backbonding with the $d_{xz}(\text{Cr})$ orbital. O and S, which have a larger electronegativity than N and P, respectively, delocalize their lone pair to a lesser extent, such that the phos-

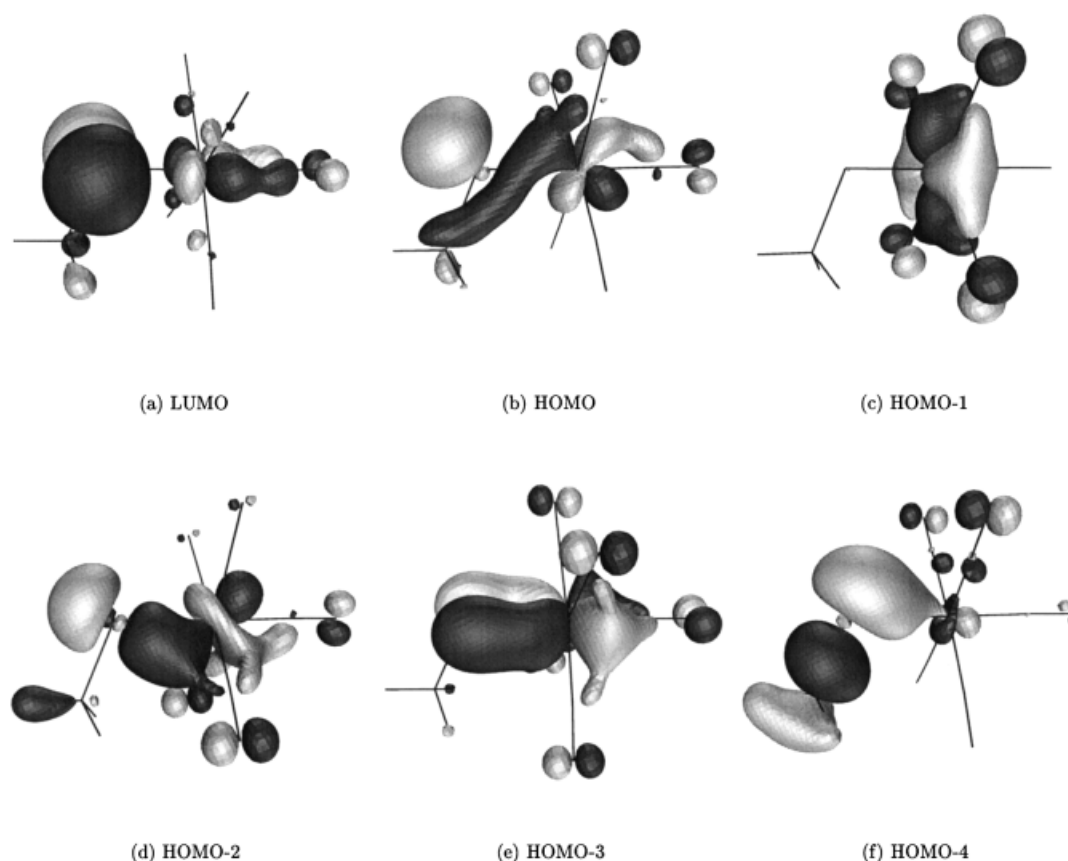


Figure 3. Molecular orbitals of the **st-A** $\text{Cr(CO)}_5\text{-PCH}_3$ molecule; the isosurfaces are plotted at a value of 0.05 a.u.

phorus p_x orbital remains more suited to backbonding with Cr in the $\text{Cr(CO)}_5\text{-POH}$ and $\text{Cr(CO)}_5\text{-PSH}$ complexes. This explains the fact that the π bond strength of $\text{Cr(CO)}_5\text{-POH}$ lies in between that of $\text{Cr(CO)}_5\text{-PCH}_3$ and $\text{Cr(CO)}_5\text{-PNH}_2$. The same applies to $\text{Cr(CO)}_5\text{-PSH}$.

For all complexes considered, the LUMO is the antibonding orbital involved in the π backbond discussed above. For $\text{R} = \text{PH}$, PCH_3 , PSiH_3 , this orbital is a simple antibonding combination of the $p_x(\text{P})$ orbital and the $d_{xz}(\text{Cr})$ orbital. However, for the internally conjugated PR fragments, this orbital is also antibonding between P and R. As an example, Figure 6 shows the LUMO of **st-A** $\text{Cr(CO)}_5\text{-PPH}_2$.

Calculated Mulliken charges show that the most electrophilic phosphinidene centers are found for $\text{Cr(CO)}_5\text{-POH}$ ($q_{\text{P}} = 0.57 e^-$) and $\text{Cr(CO)}_5\text{-PNH}_2$ ($q_{\text{P}} = 0.48 e^-$), whereas $\text{Cr(CO)}_5\text{-PSiH}_3$ has the least electrophilic P ($q_{\text{P}} = 0.14 e^-$). In general, the charge at the P center is considerably reduced upon excitation to the triplet state, due to an occupation of the LUMO, which is an orbital mainly localized on the PR unit. The charges at the Cr center are nearly constant throughout the series ($-1.5 e^-$ for singlets and $-1.3 e^-$ for triplet species). The total PR fragment charge (sum of the Mulliken charges) gives an estimate of the total charge transfer from PR to Cr(CO)_5 . It is seen that this charge transfer is largest for $\text{Cr(CO)}_5\text{-PNH}_2$ ($0.45 e^-$) and smallest for $\text{Cr(CO)}_5\text{-PSiH}_3$ ($0.20 e^-$). As shown in a further section, these compounds also have the largest and

Table 1. Various properties of complexed and free phosphinidenes

	B3LYP	$\Delta(T-S)^{[a]}$ QCISD(T) ^[b]	$\Delta E^{[c]}$ [eV]
PH	-139.2	-117.2	1.86
PCH ₃	-125.9	-108.8	2.56
POH	-76.5	-70.7	3.20
PNH ₂	-5.0	-5.0	4.14
PSiH ₃	-123.8	-107.1	1.82
PSH	-37.2	-25.5	2.90
PPH ₂	-10.5	-5.0	3.71
	B3LYP	$\Delta(T-S)^{[a]}$ CASPT2 ^[d]	B.E. [kJ/mol]
$\text{Cr(CO)}_5\text{-PH}$	24.6	36.6	137.5
$\text{Cr(CO)}_5\text{-PCH}_3$	24.4	35.8	134.9
$\text{Cr(CO)}_5\text{-POH}$	86.0	95.3	186.4
$\text{Cr(CO)}_5\text{-PNH}_2$	102.5	108.7	216.0
$\text{Cr(CO)}_5\text{-PSiH}_3$	3.8	11.2	126.9
$\text{Cr(CO)}_5\text{-PSH}$	75.2	84.4	173.4
$\text{Cr(CO)}_5\text{-PPH}_2$	30.1	23.7	137.5

^[a] $E(\text{lowest lying triplet}) - E(\text{lowest lying singlet})$ [kJ/mol]. –
^[b] Using the 6-311++G(3df,2p) basis and based on (U)MP2/6-31G(d,p) geometries given in ref.^[3]. A negative value corresponds to a triplet ground state. –
^[c] Energy difference between the LUMO of singlet PR and the d_{xz} orbital of Cr(CO)_5 . –
^[d] Including relativistic corrections.

smallest binding energy, respectively. For the triplet species, calculations show that the spin density is mainly located on both the Cr and P centers [$\rho^S(\text{Cr})$ varies from 0.61 to

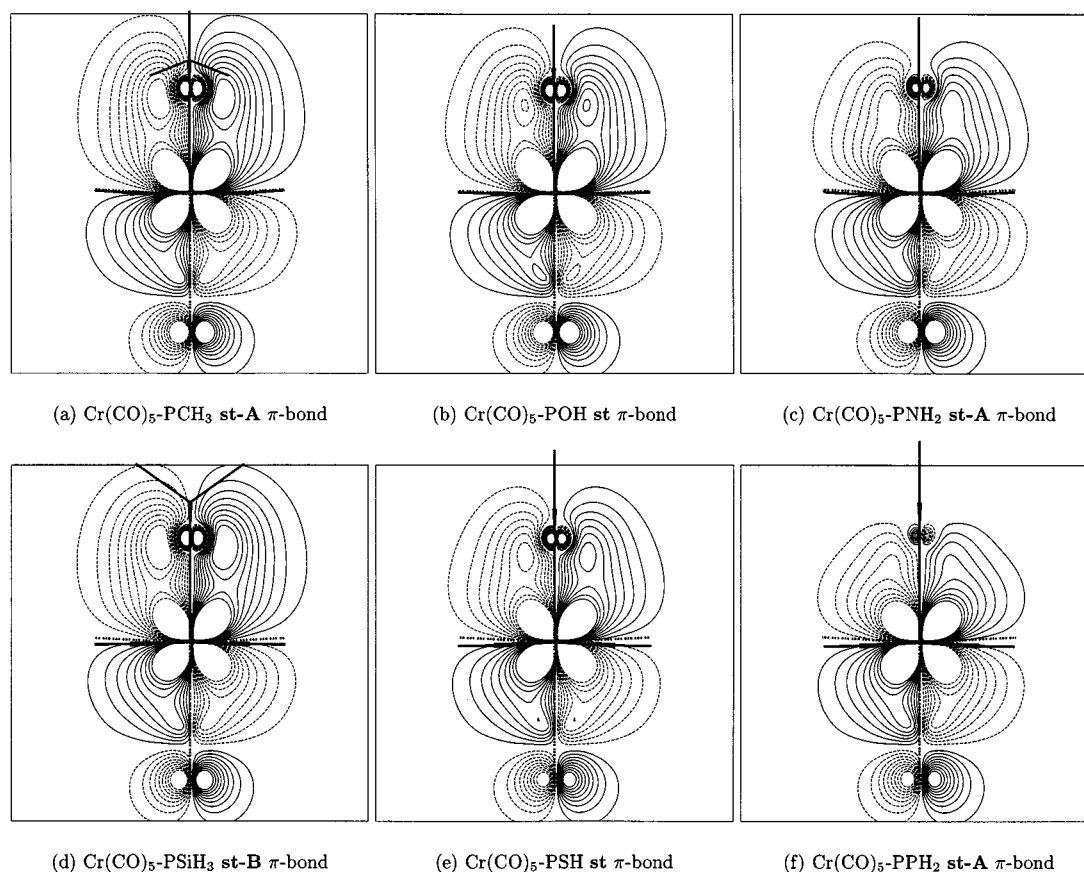
Figure 4. Contour plots of the $p_x(\text{P})-d_{xz}(\text{Cr})$ bonding orbital involved in π backdonation of the different complexes

Table 2. Selected geometrical parameters as obtained using B3LYP optimizations

		$^1\text{A}'$	$r(\text{P}-\text{Cr})$	$^3\text{A}''$	$^1\text{A}'$	$^3\text{A}''$	$r(\text{P}-\text{R})$	free PR
$\text{Cr}(\text{CO})_5-\text{PH}$	ec	2.273	2.365	1.438	1.424	$^1\Sigma^+$		1.434
	st	2.268	2.368	1.438	1.425	$^1\Sigma^-$		1.435
$\text{Cr}(\text{CO})_5-\text{PCH}_3$	ec-A	2.281	2.376	1.867	1.859	$^1\text{A}'$		1.822
	ec-B	2.282	2.378	1.861	1.861	$^3\text{A}_2$		1.861
	st-A	2.279	2.375	1.868	1.859			
	st-B	2.274	2.375	1.865	1.863			
$\text{Cr}(\text{CO})_5-\text{PNH}_2$	ec-A	2.312	2.444	1.664	1.700	$^1\text{A}_1$		1.649
	ec-B	2.269	2.405	1.768	1.696	$^3\text{A}''$		1.716
	st-A	2.303	2.432	1.666	1.703			
	st-B	2.267	2.402	1.768	1.696			
$\text{Cr}(\text{CO})_5-\text{POH}$	ec	2.242	2.394	1.660	1.668	$^1\text{A}'$		1.643
	st	2.239	2.392	1.662	1.670	$^3\text{A}''$		1.663
$\text{Cr}(\text{CO})_5-\text{PSiH}_3$	ec-A	2.293	2.343	2.291	2.253	$^1\text{A}'$		2.236
	ec-B	2.293	2.343	2.281	2.253	$^3\text{A}_2$		2.270
	st-A	2.292	2.344	2.290	2.253			
	st-B	2.288	2.344	2.283	2.256			
$\text{Cr}(\text{CO})_5-\text{PPH}_2$	ec-A	2.359	2.447	2.034	2.104	$^1\text{A}_1$		1.963
	ec-B	2.273	2.360	2.298	2.208	$^3\text{A}''$		2.210
	st-A	2.355	2.532	2.036	2.125			
	st-B	2.273	2.357	2.297	2.209			
$\text{Cr}(\text{CO})_5-\text{PSH}$	ec	2.282	2.396	2.093	2.126	$^1\text{A}'$		2.002
	st	2.279	2.400	2.095	2.127	$^3\text{A}''$		2.119

$0.99 e^-$, while $\rho^S(\text{P})$ lies between 1.23 and $1.45 e^-$. An extremely low $\rho^S(\text{P})$ value is found in $\text{Cr}(\text{CO})_5\text{-PPH}_2$, probably caused by the fact that in this molecule, a considerable amount of spin density is also found on the phosphanyl P.

A full table containing the calculated mulliken charges and spin densities is supplied as supporting information (available on the WWW under <http://www.wiley-vch.de/home/eurjic> or from the author).

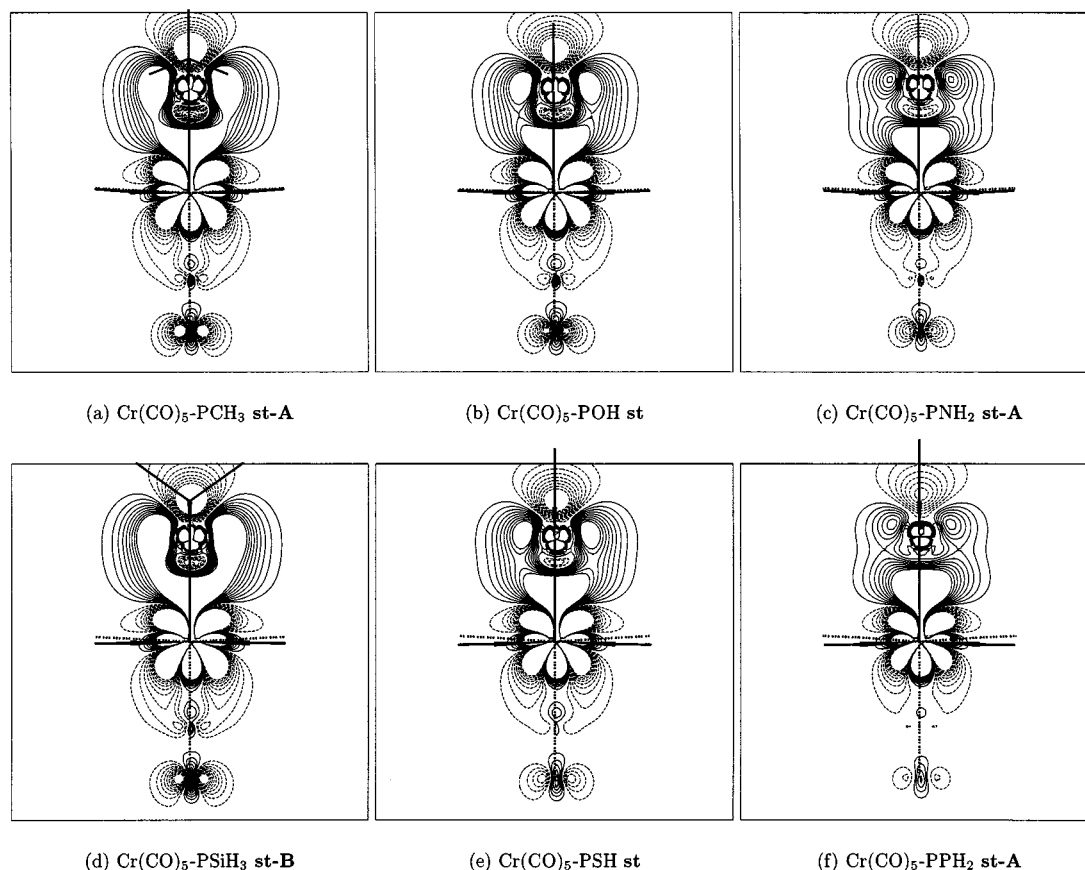


Figure 5. Density difference plots $\Delta\rho = \rho_{\text{tot}}(\text{complex}) - \{\rho_{\text{tot}}(\text{singlet PR}) + \rho_{\text{tot}}[\text{Cr}(\text{CO})_5]\}$ of the various complexes, made in the plane containing the π backbond; full lines correspond to an increase in electron density upon bond formation, dotted lines to a decrease; the maximum and minimum contour levels are 0.009 and -0.009 a.u., respectively, with intervals of 0.001 a.u.

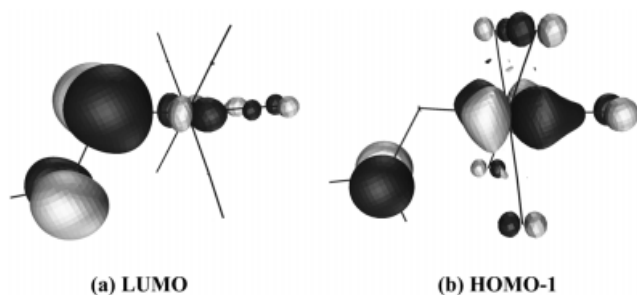


Figure 6. Some selected orbitals of the singlet **st-A** $\text{Cr}(\text{CO})_5\text{-PPH}_2$ complex

3.2 Geometries

Optimized P–R bond lengths of free phosphinidenes are listed in Table 2. The B3LYP values are consistently slightly larger than UMP2 values obtained in previous work.^[3] However, on the average, the difference in the calculated P–R distances is only about 0.01 Å, which is too small to be significant. This, together with previous work on phosphorus-containing species,^{[5][26]} shows that B3LYP is a reliable tool to obtain geometries of phosphinidenes.

Selected geometrical parameters of the complexes of interest are shown in Table 2. Included are the P–Cr and P–R distances. For singlet $\text{Cr}(\text{CO})_5\text{-PH}$, a P–Cr bond length of 2.27 Å was found, as compared to previously re-

ported values of 1.9 Å (Extended Hückel)^[13] and 2.33 Å (ROHF).^[14] For triplet $\text{Cr}(\text{CO})_5\text{-PH}$, a P–Cr distance of about 2.37 Å was found, significantly shorter than the 2.67 Å of the ROHF result reported earlier.^[14] Hence, the need for a careful geometry optimization before obtaining accurate electronic energies of these complexes is evident. In view of the successes of DFT in the last decade^[27–32] we felt that a full geometry optimization using B3LYP and the basis set specified above is a very reasonable choice.

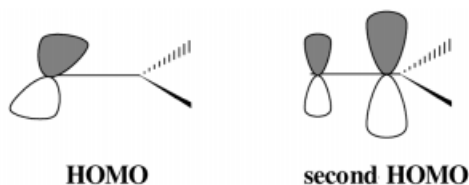
As can be seen from Table 2, in all singlet complexes the P–Cr distance is close to 2.3 Å. For the phosphane complex $\text{Cr}(\text{CO})_5\text{-PH}_3$, an experimental P–Cr distance of 2.35 Å was found.^[33] Our calculated P–Cr distances thus suggest that the P–Cr bond in the presently studied phosphinidene complexes has nearly single bond character.

The P–Cr bond lengths of the various molecules also seem to correlate with the observed π bond strengths discussed in the previous section and shown in Figures 4 and 5. As expected, the P–Cr bond becomes shorter as the π bond strength increases. Only $\text{Cr}(\text{CO})_5\text{-POH}$ and $\text{Cr}(\text{CO})_5\text{-PSH}$ do not follow this trend. However, in view of the small differences in these bond lengths, such an apparent correlation might be questionable.

Immediately apparent from Table 2 is the lengthening of the P–Cr distances following electronic transition from the $^1\text{A}'$ to the $^3\text{A}''$ state. This effect is mainly due to the exci-

tation of an electron into the LUMO, which is strongly anti-bonding between Cr and P.

Upon closer inspection of Table 2, a number of points deserve some comment. While for $\text{Cr}(\text{CO})_5\text{-PCH}_3$ and $\text{Cr}(\text{CO})_5\text{-PSiH}_3$ no significant geometry differences are found between the **A** and **B** forms, the **B** forms of $\text{Cr}(\text{CO})_5\text{-PNH}_2$ and $\text{Cr}(\text{CO})_5\text{-PPH}_2$ exhibit considerably shorter P–Cr bonds than the corresponding **A** conformations. This effect is related to the electronic structure of singlet PNH_2 and PPH_2 . In these molecules, the amino or phosphanyl π lone pair is conjugated with the empty p orbital on the phosphinidene P, resulting in a planar structure with sp^2 hybridization of the tricoordinated N and P atoms (see for instance ref. [3]). As a consequence, the second phosphinidene lone pair is found in a p orbital in the plane of the molecule. A schematic drawing of the two highest occupied molecular orbitals of both singlet PNH_2 and PPH_2 is shown in Scheme 1.



Scheme 1

The most important difference between the **A** and **B** forms of the PNH_2 or PPH_2 complexes, as can be seen from Figure 1, is not the rotation of the amino or phosphanyl group, but the fact that these groups are pyramidal in the **B** conformation, in contrast to their **A** counterparts. As such, the **B**-coordinated PNH_2 or PPH_2 phosphinidenes are no longer internally conjugated. As a consequence, the empty p -orbital on the ligating P-atom becomes more available for accepting a π backdonation of the metal, which results in a shorter P–Cr bond as compared to the **A** conformations.

One additional point has to be noted about the structures of $\text{Cr}(\text{CO})_5\text{-PNH}_2$ and $\text{Cr}(\text{CO})_5\text{-PPH}_2$. It is well known^[3] that triplet PNH_2 and PPH_2 are characterized by a pyramidal structure. The triplet **A** conformations, however, were optimized within C_s symmetry where the phosphinidene unit is prevented from becoming pyramidal. It was found that, when re-optimizing the triplet **ec-A** form in C_1 symmetry, the molecule converged to the triplet **st-B** form. As such, the triplet **A** forms of $\text{Cr}(\text{CO})_5\text{-PNH}_2$ and $\text{Cr}(\text{CO})_5\text{-PPH}_2$ might be transition states for inversion at the pyramidal phosphinidene center or rotation around the P–R bond. Since we are not able to perform vibrational analyses of these structures, the identity of the triplet **A** $\text{Cr}(\text{CO})_5\text{-PNH}_2$ and $\text{Cr}(\text{CO})_5\text{-PPH}_2$ (minimum or transition structure) remains an open question.

While for $\text{Cr}(\text{CO})_5\text{-PCH}_3$ and $\text{Cr}(\text{CO})_5\text{-PSiH}_3$ the P–R distances are systematically shorter in the triplet structures – in contrast to the situation in free phosphinidenes (Table 2) – a reverse trend is seen for $\text{Cr}(\text{CO})_5\text{-POH}$ and $\text{Cr}(\text{CO})_5\text{-PSH}$ as well as for the **A** forms of

$\text{Cr}(\text{CO})_5\text{-PNH}_2$ and $\text{Cr}(\text{CO})_5\text{-PPH}_2$. Since in these molecules the LUMO is also anti-bonding between P and R (see, for example, the LUMO in Figure 6), excitation of one electron to the LUMO causes the P–R bond to become longer with respect to the corresponding singlet form.

3.3 Relative Energies

In our previous study^[15] on $\text{Cr}(\text{CO})_5\text{-PH}$ a detailed analysis of the relative energy of the **A** and **B** forms using different methods and basis sets was performed. Here, we present only results obtained at the B3LYP and CASPT2(12/12) (including relativistic corrections) levels. The obtained relative energies are shown in Table 3. At each optimized singlet or triplet geometry, both lowest lying singlet and triplet states were calculated.

3.3.1 Conformational Behavior

We will focus on a few general characteristics of the relative energies. In every case, both B3LYP and CASPT2 methods predict a singlet staggered conformation for the ground state, except for $\text{Cr}(\text{CO})_5\text{-PNH}_2$, where CASPT2 gives a singlet **st-A** ground state, lying 1.6 kJ/mol below the **ec-A** structure, in contrast to B3LYP, which gives a singlet **ec-A** ground state, 1.2 kJ/mol below the **st-A** form. For a given conformation, the energy difference between eclipsed and staggered is rather small; the largest value amounts to 10.7 kJ/mol [$\text{Cr}(\text{CO})_5\text{-PSiH}_3$, **ec-B** – **st-B**, CASPT2]. Since frequency analyses were beyond the scope of this work, it is impossible to say whether the eclipsed forms are true minima on the potential energy surface. They might as well be transition structures for rotation of one staggered form to another. For the **A** and **B** forms of $\text{Cr}(\text{CO})_5\text{-PCH}_3$ and $\text{Cr}(\text{CO})_5\text{-PSiH}_3$ no large deviations are seen. This is, however, not true for $\text{Cr}(\text{CO})_5\text{-PNH}_2$ and $\text{Cr}(\text{CO})_5\text{-PPH}_2$. The important difference in coordination mode of PR for these complexes (**A** or **B**) has already been highlighted in the previous section on geometries. As expected, it is now confirmed that, for singlet complexes, the most favorable conformation is **A** while it turns out to be **B** for triplet forms.

3.3.2 Singlet-Triplet Energy Difference

Table 1 contains the singlet-triplet energy differences [$\Delta(T - S)$] for both free and complexed phosphinidenes. The $\Delta(T - S)$ values shown refer to $E(\text{lowest lying triplet}) - E(\text{lowest lying singlet})$. For free PR species, QCISD(T) values are also given.^[3] It is seen that, on the average, B3LYP results are about 10–20 kJ/mol higher than the QCISD(T) values. Since a detailed discussion of the variation of $\Delta E(T - S)$ throughout the PR series has already been given elsewhere,^[3] it will not be discussed any further in this work. While all free phosphinidenes considered have a triplet ground state, all their complexed counterparts have a singlet

Table 3. Relative energies of the complexed species considered

		B3LYP		CASPT2 ^[a]				B3LYP		CASPT2 ^[a]	
		¹ A'	³ A''	¹ A'	³ A''			¹ A'	³ A''	¹ A'	³ A''
<hr/>											
Cr(CO) ₅ –PH						Cr(CO) ₅ –POH					
ec	¹ A'	1.0	56.4	1.9	65.6	ec	¹ A'	1.4	118.9	2.4	113.4
	³ A''	35.0	26.3	40.7	38.9		³ A''	33.8	89.6	47.8	98.3
st	¹ A'	0.0	52.6	0.0	60.6	st	¹ A'	0.0	113.6	0.0	109.0
	³ A''	30.9	24.6	36.7	36.6		³ A''	30.3	86.0	43.3	95.3
Cr(CO) ₅ –PSH						Cr(CO) ₅ –PSH					
ec	¹ A'					ec	¹ A'	1.9	104.0	4.0	101.8
	³ A''						³ A''	31.1	77.5	47.4	87.4
st	¹ A'					st	¹ A'	0.0	99.9	0.0	96.5
	³ A''						³ A''	27.6	75.2	42.3	84.4
Cr(CO) ₅ –PCH ₃						Cr(CO) ₅ –PNH ₂					
ec-A	¹ A'	3.6	56.1	5.1	59.6	ec-A	¹ A'	–1.2	148.6	1.6	142.3
	³ A''	34.7	26.9	46.5	39.0		³ A''	31.0	119.6	51.7	130.4
ec-B	¹ A'	2.9	61.1	8.	68.2	ec-B	¹ A'	116.1	144.1	97.0	136.9
	³ A''	38.0	28.2	52.9	42.6		³ A''	156.3	102.2	148.5	111.2
st-A	¹ A'	0.0	51.1	0.0	53.5	st-A	¹ A'	0.0	146.3	0.0	140.1
	³ A''	28.2	24.4	39.0	35.8		³ A''	29.3	119.5	46.3	129.3
st-B	¹ A'	0.0	59.5	0.9	63.1	st-B	¹ A'	113.3	140.9	91.9	131.9
	³ A''	33.4	28.3	45.6	40.4		³ A''	153.5	101.3	144.3	108.7
Cr(CO) ₅ –PSiH ₃						Cr(CO) ₅ –PPH ₂					
ec-A	¹ A'	6.0	29.5	5.8	30.0	ec-A	¹ A'	0.1	148.4	2.9	142.9
	³ A''	35.3	4.2	45.3	13.3		³ A''	28.3	123.7	50.3	130.1
ec-B	¹ A'	6.0	33.5	10.7	38.2	ec-B	¹ A'	33.3	65.2	18.0	53.8
	³ A''	38.5	6.0	50.2	15.9		³ A''	70.1	31.9	61.1	27.3
st-A	¹ A'	2.9	27.3	0.5	25.3	st-A	¹ A'	0.0	145.5	0.0	137.8
	³ A''	30.3	3.8	38.7	11.2		³ A''	32.9	128.4	52.7	162.7 ^[b]
st-B	¹ A'	0.0	30.6	0.0	30.6	st-B	¹ A'	28.8	60.5	11.1	47.1
	³ A''	31.0	5.0	41.0	13.7		³ A''	63.6	30.1	53.0	23.7

^[a] Including relativistic corrections. – ^[b] CASSCF frozen up to $3p(\text{Cr})$.

ground state. For the complexed forms, B3LYP apparently underestimates the CASPT2 values. It is seen that the larger the absolute value of the singlet-triplet splitting of the free PR, the smaller this quantity for $\text{Cr}(\text{CO})_5\text{--PR}$. One exception to this rough tendency, is $\text{Cr}(\text{CO})_5\text{--PPH}_2$. Based upon the analysis of the π bond strength of the previous section, we can tentatively say that in this case, the singlet form is less stable (relative to other complexes) due to its very weak π backbonding. Note, however, that a direct comparison between $\Delta(T - S)$ values for free and complexed phosphinidenes might not be legitimate, since in free phosphinidenes it concerns an excitation within PR orbitals, while in complexed phosphinidenes, the excitation is from the HOMO, which is an orbital with mainly $d_{yz}(\text{Cr})$ character, to the LUMO, having mainly $p_x(\text{P})$ character.

At this point, the high relative energy of triplet **st-A** $\text{Cr}(\text{CO})_5\text{--PPH}_2$ should be noted. As explained in the section on the choice of the active space, problems were encountered for this molecule. The most probable reason is the relatively long P–Cr bond length obtained by B3LYP for this molecule.

In summary, in order to obtain $\text{Cr}(\text{CO})_5\text{--PR}$ complexes with singlet ground states well below the triplet state, the phosphinidene ligand should have an internally stabilized singlet state through π donation of the R group. However, if this internal π donation becomes too strong, the P-center is no longer sufficiently able to accept π donation from the $\text{Cr}(\text{CO})_5$ fragment. As such, two opposing effects are present, yielding – for the series presently studied – an opti-

mum for $\text{Cr}(\text{CO})_5\text{--PNH}_2$. The latter complex has a $\Delta(T - S)$ value of 108.7 kJ/mol at the CASPT2 level.

3.3.3 Overall Stability

The main parameter to judge the overall stability of a complex is the binding energy listed in Table 1, which is defined as $\text{B.E.} = E[\text{Cr}(\text{CO})_5\text{--PR}] - \{E(\text{triplet PR}) + E[\text{Cr}(\text{CO})_5]\}$. As discussed in our previous study^[15] on $\text{Cr}(\text{CO})_5\text{--PH}$, CASPT2(12/12) turns out to be somewhat problematic for the B.E. of this type of compounds. Upon dissociation of the phosphinidene ligand, the (12/12) space reduces to a (10/10) space on the $\text{Cr}(\text{CO})_5$ fragment and a (2/2) space on the PR unit. A (2/2) space on triplet PH, in fact, is a simple ROHF calculation. Considerably different CASPT2 energies were obtained when instead a (6/10) space on PH was used, including all valence orbitals and the $3d(\text{P})$ orbitals (about 34 kJ/mol). After correcting the CASPT2(12/12) binding energy for the shortcomings of the (2/2) active space and for basis set superposition errors (BSSE), values very close to the B3LYP results were obtained. Therefore, we present here only the B.E. obtained using B3LYP. The $\text{Cr}(\text{CO})_5\text{--PNH}_2$ complex has a B.E. of 216 kJ/mol, followed by $\text{Cr}(\text{CO})_5\text{--POH}$ (186 kJ/mol) and $\text{Cr}(\text{CO})_5\text{--PSH}$ (173 kJ/mol). Then the B.E. drops by about 36 kJ/mol for the remaining complexes, with $\text{Cr}(\text{CO})_5\text{--PSiH}_3$ having the lowest B.E. of 127 kJ/mol. It is thus seen that the complex having the highest $\Delta(T - S)$ also has the highest B.E.

4 Concluding Remarks

Cr(CO)₅ complexes of differently substituted phosphinidenes (PR, R = H, CH₃, SiH₃, NH₂, PH₂, OH, and SH) have been studied by high level ab initio (CASPT2 + relativistic corrections) and density functional (B3LYP) methods. It is shown that the P–Cr bond is essentially formed by a ligand-to-metal σ charge transfer; π backbonding is also manifested in the complexes of PH, PCH₃, and PSiH₃, but its importance systematically decreases in Cr(CO)₅–POH, Cr(CO)₅–PSH, and Cr(CO)₅–PNH₂, and is almost absent in Cr(CO)₅–PPH₂. Both B3LYP and CASPT2 methods show that all complexes have a singlet, staggered ground state conformation. There is only one case [Cr(CO)₅–PNH₂] where B3LYP predicts a different ground state conformation from CASPT2, but the energy difference is rather small – the eclipsed-staggered energy differences are small in general. One of the most intriguing parameters, both from an experimental and theoretical point of view, is the singlet-triplet energy difference [$\Delta(T - S)$] in these complexes. While the largest gap is found for Cr(CO)₅–PNH₂ amounting to 103 kJ/mol at the B3LYP level and 109 kJ/mol at the CASPT2 level, Cr(CO)₅–PSiH₃ exhibits the smallest gap of only 4 kJ/mol at B3LYP and 11 kJ/mol at CASPT2. The binding energies (B.E.) for P–Cr bond cleavage, as computed by the B3LYP method, show a similar behavior; the largest value is 216 kJ/mol for Cr(CO)₅–PNH₂, while Cr(CO)₅–PSiH₃ has the smallest B.E. of 127 kJ/mol. The trends in $\Delta(T - S)$ and B.E. can be understood in terms of electronic structure.

The qualitative trends emphasized by CASPT2 calculations are well reproduced by the B3LYP method and, in most cases, a quantitative agreement between the two methods is found as well.

Acknowledgments

We are indebted to the Fund for Scientific Research (FWO Vlaanderen) and “Geconcerteerde Onderzoeksacties” (GOA) for continuing support and the K. U. Leuven Computing Centre for generous allocation of computer time.

- [1] X. Li, S. I. Weisman, T.-S. Lin, P. P. Gaspar, A. H. Cowley, A. I. Smirnov, *J. Am. Chem. Soc.* **1994**, *116*, 7899.
- [2] F. Mathey, *Multiple bonds and low coordination in phosphorus chemistry*, Georg Thieme Verlag, New York, **1990**.
- [3] M. T. Nguyen, A. Van Keer, L. G. Vanquickenborne, *J. Org. Chem.* **1996**, *61*, 7077.
- [4] M. T. Nguyen, A. Van Keer, L. A. Eriksson, L. G. Vanquickenborne, *Chem. Phys. Lett.* **1996**, *254*, 307.
- [5] M. T. Nguyen, S. Creve, L. G. Vanquickenborne, *J. Chem. Phys.* **1996**, *105*, 1922.
- [6] M. T. Nguyen, A. Van Keer, L. G. Vanquickenborne, *J. Organomet. Chem.* **1997**, *529*, 3.
- [7] T. P. Hamilton, A. G. Willis, S. D. Williams, *Chem. Phys. Lett.* **1995**, *246*, 59.
- [8] V. Parasuk, C. J. Cramer, *Chem. Phys. Lett.* **1996**, *260*, 7.
- [9] F. Mercier, B. Deschamps, F. Mathey, *J. Am. Chem. Soc.* **1989**, *111*, 9098.
- [10] A. Marinetti, F. Mathey, *Organometallics* **1984**, *3*, 456.
- [11] B. Wang, K. Lammerstma, *J. Am. Chem. Soc.* **1994**, *116*, 10486.
- [12] G. Trinquier, G. Bertrand, *Inorg. Chem.* **1985**, *24*, 3842.
- [13] D. Gonbeau, G. Pfister-Guillouzo, A. Marinetti, F. Mathey, *Inorg. Chem.* **1985**, *24*, 4133.
- [14] J. –G. Lee, J. E. Boggs, A. H. Cowley, *Polyhedron* **1986**, *5*, 1027.
- [15] S. Creve, K. Pierloot, M. T. Nguyen, *Chem. Phys. Lett.* **1998**, *285*, 429.
- [16] K. B. Dillon, F. Mathey, J. F. Nixon, *Phosphorus: the carbon copy. From organophosphorus to phospho-organic chemistry*, Wiley, Chichester, **1998**.
- [17] A. D. Becke, *J. Chem. Phys.* **1993**, *89*, 5648.
- [18] C. Lee, W. Yang, R. G. Parr, *Phys. Rev. B* **1988**, *37*, 785.
- [19] A. Schäfer, H. Horn, R. Ahlrichs, *J. Chem. Phys.* **1992**, *97*, 2571.
- [20] A. J. H. Wachters, *J. Chem. Phys.* **1970**, *52*, 1033.
- [21] P. J. Hay, *J. Chem. Phys.* **1977**, *66*, 4377.
- [22] K. Pierloot, B. Dumez, P.-O. Widmark, B. O. Roos, *Theor. Chim. Acta* **1995**, *90*, 87.
- [23] IBM Corporation, *Mulliken, version 1.1.0*, **1994**.
- [24] K. Anderson, M. R. A. Blomberg, M. P. F. Fulsher, V. Kell, R. Lindh, P.-A. Malmqvist, J. Noga, J. Olsen, B. O. Roos, A. J. Sadlej, P. E. M. Siegbahn, M. Urban, *MOLCAS-4.0*, University of Lund, Sweden, **1996**.
- [25] B. J. Persson, B. O. Roos, K. Pierloot, *J. Chem. Phys.* **1994**, *101*, 6810.
- [26] M. T. Nguyen, S. Creve, L. G. Vanquickenborne, *J. Phys. Chem. A* **1997**, *101*, 3174.
- [27] T. Ziegler, *Chem. Rev.* **1991**, *91*, 651.
- [28] G. Rauhut, P. Pulay, *J. Phys. Chem.* **1995**, *99*, 3093.
- [29] P. J. Hay, *J. Phys. Chem.* **1996**, *100*, 5.
- [30] J. Andzelm, J. Baker, A. Scheier, M. Wrinn, *Int. J. Quant. Chem.* **1995**, *56*, 733.
- [31] V. G. Malkin, O. L. Malkina, L. A. Eriksson, D. R. Salahub, *Modern Density Functional Theory: A Tool for Chemistry*, vol. 2, Elsevier, Amsterdam, **1995**.
- [32] M. Kaupp, V. G. Malkin, O. L. Malkina, D. R. Salahub, *Chem. Eur. J.* **1996**, *2*, 24.
- [33] G. Huttner, S. Schelle, *J. Organomet. Chem.* **1973**, *47*, 383.

Received July 29, 1998
[I98254]